Molecular Autism

Deviation from normative brain development is associated with symptom severity in autism spectrum disorder

Birkan Tunç[1,2,3,4*] , Lisa D. Yankowitz[1,5], Drew Parker[6], Jacob A. Alappatt[6], Juhi Pandey[1,3], Robert T. Schultz[1,3,7†] and Ragini Verma[4,6†]

Abstract

Background: Autism spectrum disorder (ASD) is a heterogeneous neurodevelopmental condition. The degree to which the brain development in ASD deviates from typical brain development, and how this deviation relates to observed behavioral outcomes at the individual level are not well-studied. We hypothesize that the degree of deviation from typical brain development of an individual with ASD would relate to observed symptom severity.

Methods: The developmental changes in anatomical (cortical thickness, surface area, and volume) and diffusion metrics (fractional anisotropy and apparent diffusion coefficient) were compared between a sample of ASD ($n = 247$) and typically developing children (TDC) ($n = 220$) aged 6–25. Machine learning was used to predict age (brain age) from these metrics in the TDC sample, to define a normative model of brain development. This model was then used to compute brain age in the ASD sample. The difference between chronological age and brain age was considered a developmental deviation index (DDI), which was then correlated with ASD symptom severity.

Results: Machine learning model trained on all five metrics accurately predicted age in the TDC ($r = 0.88$) and the ASD ($r = 0.85$) samples, with dominant contributions to the model from the diffusion metrics. Within the ASD group, the DDI derived from fractional anisotropy was correlated with ASD symptom severity ($r = -0.2$), such that individuals with the most advanced brain age showing the lowest severity, and individuals with the most delayed brain age showing the highest severity.

Limitations: This work investigated only linear relationships between five specific brain metrics and only one measure of ASD symptom severity in a limited age range. Reported effect sizes are moderate. Further work is needed to investigate developmental differences in other age ranges, other aspects of behavior, other neurobiological measures, and in an independent sample before results can be clinically applicable.

Conclusions: Findings demonstrate that the degree of deviation from typical brain development relates to ASD symptom severity, partially accounting for the observed heterogeneity in ASD. Our approach enables characterization of each individual with reference to normative brain development and identification of distinct developmental subtypes, facilitating a better understanding of developmental heterogeneity in ASD.

Keywords: Autism, Brain development, Heterogeneity, Symptom severity, Machine learning, Normative modeling

* Correspondence: tuncb@email.chop.edu
†Robert T. Schultz and Ragini Verma contributed equally to this work.
[1]Center for Autism Research, The Children's Hospital of Philadelphia, Philadelphia, PA 19104, USA
[2]Department of Biomedical and Health Informatics, The Children's Hospital of Philadelphia, Philadelphia, PA 19104, USA
Full list of author information is available at the end of the article

Background

Autism spectrum disorder (ASD) is a heterogeneous neurodevelopmental condition associated with atypical trajectories of brain anatomy, function, and connectivity, distinguishing it from typical development [1–8]. Although the exact details of developmental changes in ASD vary across individual studies, one fact is well established in the literature: ASD has a complex and dynamic neurobiological mechanism(s), with the disorder-related changes in the brain showing variations across ages [9, 10]. For example, head circumference and brain imaging data suggest that individuals later diagnosed with ASD have typical brain volume from birth through 6 months of age [11, 12]. This is followed by a period of accelerated growth, resulting in larger brains by age two [13, 14]. Evidence regarding brain volume differences in older children and adolescents with ASD is mixed, although differences in brain volume may be smaller than in toddlerhood [15–17]. Thus, consideration of the development is crucial to understanding the neurobiology of ASD.

The differential development of ASD pathology suggests that the *expected* neuroanatomical features of individuals with ASD should be adjusted based on their ages; that is, the exact nature of atypicality in ASD and the direction of deviation from typicality (e.g., bigger brains or smaller brains) may change with age. Furthermore, individuals with ASD also show variations within their age groups and follow different developmental trajectories [18, 19], and even make shifts between various possible trajectories at different ages [20]. Therefore, a comprehensive understating of heterogeneous behavioral impairments in ASD requires studies that can elucidate developmental blueprints of the brain and identify distinct developmental subtypes of ASD associated with divergent behavioral profiles.

The ASD-related developmental changes on the anatomical features of the brain such as volume, cortical surface area, and cortical thickness have been extensively studied [10, 13, 21–23]. For example, the presence of atypical brain enlargement in infancy and early childhood is well documented [14, 23–25]. One aspect of brain development that needs to be further investigated is the interaction between brain anatomy and other neurobiological features related to brain connectivity (e.g., white matter tissue characteristics). In the last decade, brain connectivity alterations (e.g., disruption in diffusion metrics) have emerged as candidate biomarkers in [26–34], owing to recent advances in diffusion MRI (dMRI) [35, 36]. While there exist many neurobiological findings on diffusion-related alterations in ASD, their developmental characteristics remain unclear. Even less is known about how ASD-related developmental differences, both anatomical and diffusion-related, are linked to heterogeneous behavioral profiles.

A comprehensive understanding of developmental heterogeneity in ASD necessitates insights into typical brain development and investigations on individual-level deviations from typical development. Recent normative modeling techniques [37] can facilitate such investigations by modeling brain maturation using a healthy sample, and then quantifying individual differences from this normative model. Within this framework, disorders are conceptualized as extreme values of quantitative biological measures (e.g., neuroimaging metrics) or deviations from normative functioning, enabling a dimensional analysis to study heterogeneous presentations [37, 38].

Normative modeling techniques use prediction algorithms (e.g., machine learning) to model relationship between biological measures and other clinically relevant variables. Once the prediction algorithm is trained using a healthy sample to define a normative model, it is then applied to a patient sample to quantify deviations of individuals from this normative model. These techniques usually use two alternative approaches regarding the directionality of the relationship between biological measures and other clinically relevant variables. One approach is to predict a given single biological measure (e.g., cortical thickness of a specific brain region) from clinical or demographic variables (e.g., age, sex) [38], whereas in the second approach, the mapping is inverted and a clinical or demographic variable is predicted from multiple biological measures (e.g., cortical thickness across all brain regions) [39]. Both approaches can be utilized in neuroimaging studies and have their own advantages and drawbacks.

The first approach allows identification of regional deviations that may change across individuals [40], providing a clear picture on how a single behavioral outcome can be a result of distinct alteration patterns in the brain [41]. The second approach, mostly known as a *brain age* approach, fuses information from multiple regions to predict the chronological age of individuals, implicitly defining normative maturation patterns. Brain age models, while limiting region-specific interpretations, use multivariate machine learning techniques to better capture complex interactions between brain regions during development [42, 43], as well as the interplay between different modalities such as anatomical and diffusion metrics. This approach yields a summary score of multimodal brain development (brain age) and enables defining an index of deviation for each individual (i.e., difference between brain age and chronological age) [39]. Moreover, one may easily model the relationship between this individual-level index and the behavioral differences related to the disorder.

In this study, within a large dataset of children and young adults ($N = 467$, age = 6–25 years, 247 with ASD),

Tunç et al. Molecular Autism   (2019) 10:46

Page 3 of 14

we used brain age approach explained above and developed an individual-level measure of multimodal brain development, called *developmental deviation index* (DDI), to parse behavioral heterogeneity in ASD. In order to define a normative model of brain development, we investigated developmental changes in anatomical (cortical volume, cortical surface area, and cortical thickness) and diffusion metrics (fractional anisotropy [FA] and apparent diffusion coefficient [ADC]) of the brain. The normative model, trained using typically developing children (TDC), was then used to study the relationship between individual-level deviation from the normative model and disorder symptom severity in ASD. We hypothesized that the affected participants with a positive DDI (i.e., brain age > chronological age) would manifest less symptom severity compared with the affected participants with a negative DDI (i.e., brain age < chronological age). Our approach enables characterization of each individual with reference to normative brain development and identification of distinct developmental subtypes, facilitating a better understanding of developmental heterogeneity in ASD. This in turn may lead to improved assessment of developmental or treatment-related change, to targeted and individualized treatment planning, and eventually to a true precision medicine approach in ASD.

Methods

Participants

Data collection was performed at the Center for Autism Research (CAR) at Children's Hospital of Philadelphia (CHOP), from February 2009 to February 2013. Data collection and use was approved by the institutional review board (IRB) at CHOP and the University of Pennsylvania. Individuals with a community diagnosis of an ASD were recruited in part through autismMatch (https://autismmatch.org). Diagnoses were confirmed by the clinical core at CAR, using DSM-IV-TR criteria [44], informed by Autism Diagnostic Observation Schedule (ADOS) [45] and Autism Diagnostic Interview-Revised [46], and expert consensus clinical judgment by two independent psychologists following Collaborative Programs of Excellence in Autism diagnostic guidelines. Children with known genetic conditions associated with ASD were excluded from the study. The symptom severity of participants was assessed using ADOS calibrated severity score (CSS) [47], and the cognitive ability (IQ) was assessed with the Differential Abilities Scale, Second Edition [48]. The details on the dataset ($N = 467$, Age = 6–25 years) are given in Table 1.

Image acquisition and processing

T1-weighted anatomical images were acquired on a Siemens 3 T wide-bore Magnetom Verio Tim scanner with a 12-channel head coil and a Siemens MPRAGE sequence ($0.8 \times 0.8 \times 0.9$ mm, TR = 1900, TE = 2.54, flip angle = 9). Images were N3 bias corrected with ANTS [49] and brain extracted with LABEL [50]. Measures of cortical volume, cortical surface area, and cortical thickness were derived using the Freesurfer image analysis suite version 5.3.0 [51], for each region in the Desikan-Killiany cortical atlas [52] (34 cortical regions of interest per hemisphere).

Diffusion characteristics of the brain tissue were assessed by diffusion weighted imaging (DWI). The DWI dataset was acquired in three epochs on the same scanner (Siemens Verio 3 T). In the first epoch, DWI was acquired using a monopolar sequence, with repetition time(TR)/echo time (TE) = 14,000/70 ms. In the second epoch, DTI was acquired at TR/TE = 11,000/75 ms using a monopolar+ sequence. In the third, DTI was acquired at TR/TE = 11,000/76 ms using a monopolar sequence. All data was acquired with an image resolution of $2 \times 2 \times 2$ mm, collecting 30 directions with b-value = 1000 s/mm^2 and one $b = 0$ image. We verified that there were no significant difference between scanning epochs in terms of DTI metrics of fractional anisotropy (FA) and apparent diffusion coefficient (ADC), as well as participant age, IQ, and ADOS severity. The diffusion metrics did not show any significant difference across the acquisition protocols, neither in different tissue types, nor in the whole brain.

In order to quantify the MRI motion, we used the technique proposed in [53]. We used "eddy" from FSL 5.0 to estimate volume-to-volume rotations and translations. These measures were then transformed from radian angles to displacement in millimeters, from which the root mean square displacement was computed.

Table 1 Demographics and clinical profile of participants. With *ADOS*, social affect (SA) and restricted and repetitive behaviors (RRB) scores are listed

Diagnosis	Age Min-Max, Mean (Std)	Sex	IQ Mean	ADOS Mean
TDC ($n = 220$)	6.26–25.63 13.06 (4.12)	Male, 161 Female, 59	Verbal, 114.48 Nonverbal, 108.09 Total, 112.81	SA, 2.05 RRB, 2.50 Total, 1.70
ASD ($n = 247$)	6.36–25.87 12.85 (3.52)	Male, 203 Female, 44	Verbal, 100.63 Nonverbal, 100.24 Total, 100.23	SA, 6.76 RRB, 7.09 Total, 6.85

In the final dataset, 467 participants had at least one imaging modality (anatomical and diffusion) that passed our QA pipelines (see Additional file 1: Section S1 for details). Three hundred forty-nine participants had reliable diffusion metrics, and 415 participants had reliable anatomical metrics. Two hundred sixty-one participants had both diffusion and anatomical metrics acquired during the same session. When training a machine learning model using a single modality, we used all available data for that modality (i.e., 349 for diffusion and 415 for anatomical). For the combined model, we used only 261 participants who had both modalities.

Multivariate-multimodal analysis using machine learning

We used support vector regression (SVR) [54] for predicting chronological age of participants from diffusion and anatomical metrics. SVR is commonly used in brain imaging studies [39, 55] due to its superiority in interpretation of outcomes, as compared with more complex methods (e.g., deep learning models) that obscure neurobiological interpretations on inner workings of the model. In order to facilitate insights regarding how regional metrics contribute into age prediction, we used a linear kernel with SVR, which assigns weights to features (i.e., regional values) reflecting their contributions. We used the SVR package with default settings implemented in Scikit-learn library [56] for Python [57].

We trained six SVR models to predict the age of participants, five with individual metrics (volume, surface area, thickness, FA, ADC) and one with combined metrics. An individual model using only a diffusion metric had 176 features corresponding to regional mean FA or ADC values. For individual models using only anatomical metrics, there were 68 features corresponding to regional mean volume, thickness, or surface area. Thus, the combined model using all modalities had 556 features. We did not use an external feature selection procedure, and the importance of features was determined using the feature weights as calculated by the SVR algorithm.

Each SVR model was trained using only the TDC sample to define a normative model of development. Prediction accuracy of the normative models was assessed using 10-fold cross-validation, repeated 1000 times in randomized order. In each fold, 10% of the data was kept for testing and the rest was used for training the SVR model. The ages of the participants in the test sample were then predicted using the trained model. This was repeated (10-fold) to use all participants once in the test sample, and the accuracy was calculated as Pearson correlation between predicted and actual age. Finally, the entire procedure was repeated 1000 times (i.e., 1000 times 10-folds), after randomly changing the order of participants, yielding 1000 Pearson r values. We reported the mean accuracy and 95% confidence interval using this distribution of r values.

We also demonstrated that the reported results are not model-dependent by repeating all analyses using two more regression models, namely Lasso and Bayesian regression. The use of Bayesian regression, by providing metrics on prediction uncertainty, also allowed us to incorporate into the model uncertainty induced by the availability of data across ages and variation across people in the training sample, to better capture individual differences [37, 38]. Results as reported in Additional file 1: Section S3 were highly similar to the original results reported below, demonstrating that our results are not model-dependent, nor driven by unaccounted uncertainty.

Developmental deviation index

The normative age prediction model (SVR), trained using the TDC sample, was used to predict ages of participants with ASD, yielding their *brain age*. We calculated the difference between predicted age (brain age) and the chronological age for each participant with ASD, as an index of deviation from normative development, called *developmental deviation index* (DDI). When using a linear regression model, the regression towards the mean effect [58] results in younger ages being systematically overestimated and older ages being systematically underestimated. Therefore, the difference between brain age and chronological age is expected to be correlated with chronological age, obscuring real developmental deviation [59]. Thus, we adjusted the DDI for the regression towards the mean effect, by regressing out the chronological age from the DDI values [39]. For ease of interpretation, DDI was normalized to have a mean of 0 and standard deviation of 1.

Statistical metrics

The correlation between age and neurobiological metrics (FA, ADC, surface area, volume, thickness) was calculated using Pearson correlation coefficient r. The statistical significance of the difference between the TDC and ASD groups, in terms of correlation between age and the neurobiological metrics, was assessed using Fisher r to z transformation. We only tested for regions whose age correlation was significant ($p < 0.05$) in both groups.

The correlation between the DDI and the ADOS severity was calculated using Spearman's rank correlation coefficient due to the ordinal nature of ADOS severity scores. The effect size of difference in ADOS severity scores, for the same reason, was reported using common-language effect size [60]. The common-language effect size is the probability of having higher/lower severity in one of the groups, and is easy to interpret since it reports a probability value [61]. The

Cohen's *d* values were also reported for the sake of completeness, but they should be interpreted carefully, as ADOS severity scores are not distributed normally.

The false discovery rate (FDR) technique [62] was used for multiple comparisons correction. When studying correlations between age and individual metrics, FDR was used for each metric individually, correcting for multiple comparisons due to multiple brain regions.

The 95% confidence intervals (CI) for Pearson *r* values were calculated using Fisher *r* to *z* transformation. With the SVR model of the normative age prediction (using the TDC sample), we had 1000 *r* values (1000 times 10-fold cross validation); thus, we are able to estimate the standard error of the *z* distribution from those 1000 values. In other cases (e.g., testing accuracy with the ASD sample), the standard error was estimated based on sample size $(1/\sqrt{N-3})$.

In order to test the robustness of our findings against MRI motion and IQ differences, we fitted an ordinal regression model to predict ADOS severity scores using the DDI, MRI motion, and total IQ (Severity ~ DDI + Motion + IQ). We used the *ordinal* package [63] in R [64].

Results

We first investigated developmental changes in anatomical and diffusion metrics of the brain, both in typical development and in ASD, in order to elucidate diverse effects of age on those metrics across different brain tissues and regions. We studied developmental alteration/similarity in ASD as compared with TDC. We then defined a normative model of multimodal brain development by fusing diverse age affects across brain regions, using a multivariate machine learning model. Finally, we studied how individual-level deviation from this normative model related to behavioral variation in ASD. Specifically, we defined distinct subgroups of ASD, each having different deviation from the normative model and compared them in terms of symptom severity values. We also demonstrated a dimensional relationship between individual-level deviation and disorder symptom severity.

Patterns of regional brain maturation

We studied how anatomical and diffusion metrics of the brain change with age within the TDC sample, to elucidate normative patterns of brain maturation. We observed divergent effects of age on diffusion metrics across tissue types, as seen in Fig. 1, with increase in certain tissue types and decrease or no change in others. The effects of age were more homogenous on anatomical metrics. The cortical volume and cortical thickness, on average, decreased in both hemispheres. The cortical

surface area, on average, did not change with age in either of hemispheres. Details are given in Additional file 1: Section S2. The effects of maturation were heterogeneous across brain regions as illustrated in Fig. 2a, with correlation between age and all metrics showing variations across regions.

Overall patterns of maturation in the ASD sample were very similar to that of the TDC sample for all anatomical and diffusion metrics as shown in Fig. 2b and Additional file 2: Figure S1. In ASD, the absolute correlation values were slightly decreased with FA, ADC, and cortical thickness (see Additional file 3: Table S1 for details). Nevertheless, after multiple comparison correction, results remained significant only with ADC metric and only in the seven regions listed in Additional file 3: Table S1, suggesting an agreement between maturation patterns in TDC and in ASD.

Multivariate-multimodal brain development

The SVR model using all metrics in combination achieved a high 10-fold cross-validation accuracy in predicting age (brain age) within the TDC sample (Pearson correlation between chronological and brain age, *r* = 0.88, CI = [0.87–0.89]). The feature weights that reflect contribution of regional metrics towards age prediction in the TDC sample are given in Fig. 3 for the top 30 features. As can be seen in the Fig. 3a, diffusion metrics (FA and ADC) were dominant in predicting age, representing 23 of the top 30 features. Similarly, diffusion metrics, in general, compared with anatomical metrics, achieved higher cross-validated prediction accuracy when normative models were trained using individual metrics (ADC: *r* = 0.87, CI = [0.85–0.88]; FA: *r* = 0.80, CI = [0.78–0.81]; thickness: *r* = 0.79, CI = [0.78–0.80]; volume: *r* = 0.66, CI = [0.64–0.68]; area: *r* = 0.22, CI = [0.16–0.27]).

The normative models achieved very high testing accuracy when tested with the ASD sample, both using all metrics in combination (Pearson *r* = 0.85, CI = [0.80–0.89]) and using individual metrics (ADC: *r* = 0.78, CI = [0.72–0.83]; FA: *r* = 0.76, CI = [0.69–0.82]; thickness: *r* = 0.79, CI = [0.74–0.84]; volume: *r* = 0.59, CI = [0.50–0.67]; area: *r* = 0.26, CI = [0.13–0.38]).

Deviation from normative development and ASD severity

Among six SVR models (five individual models and one combined model), only one model, using the FA metric only, revealed significant correlation between the DDI and the symptom severity. This remained significant after multiple comparison correction for the six models. Below we report results using the FA model; others can be seen in Additional file 4: Table S2.

A total of 176 participants with ASD had both diffusion imaging and ADOS calibrated severity score. In
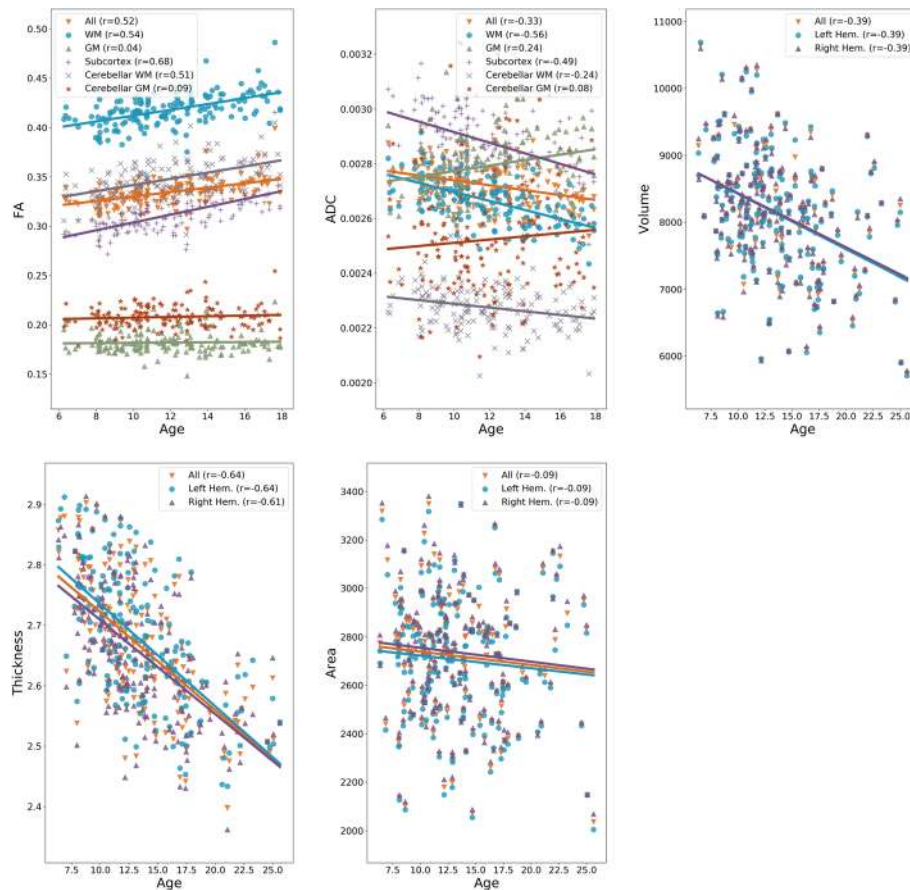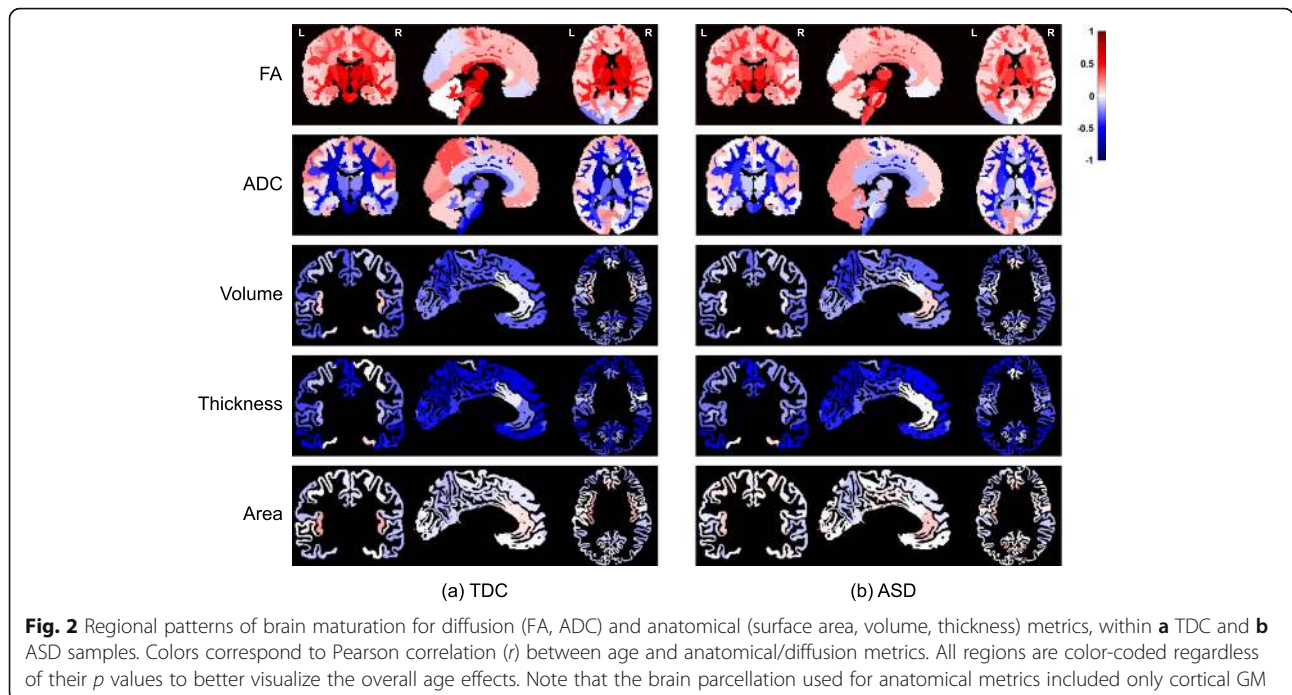
Fig. 1 Global patterns of normative brain maturation for diffusion (FA, ADC) and anatomical (surface area, volume, thickness) metrics. Note that the brain parcellation used for anatomical metrics included only cortical GM. Heterogeneous effects of age on diffusion metrics are observed across tissue types. All anatomical metrics decline with age, with a similar trend in both hemispheres

order to investigate the developmental heterogeneity in ASD, we defined three subgroups, as listed in Table 2, namely (1) Advanced group ($n = 19$) including participants with DDI > = 1, (2) Delayed group ($n = 27$) including participants with DDI < = – 1, and (3) Balanced group ($n = 26$) including participants with – 0.2 < DDI < 0.2. Note that DDI values were normalized to have a standard deviation of 1. The threshold for the Balanced group was chosen to have a sample size (∼ 25) that is comparable to the other two groups. A notable hierarchy was observed among the three subgroups (Fig. 4) in terms of their symptom severity (Delayed > Balanced > Advanced; Kruskal-Wallis H-test statistic = 7.84, p = 0.0198) with a substantial effect size between the Delayed and Advanced subgroups (Cohen's d = 1.01, common-language effect size = 0.74; Mann-Whitney test statistic = 380.5, p = 0.0051). The difference between the Delayed and Advanced subgroups was robust to the choice of the DDI thresholds as illustrated in Fig. 4c. There was no significant group difference between the two groups in terms of age (Cohen's d = – 0.09,

common-language effect size = 0.45; Mann-Whitney test statistic = 241.0, p = 0.5397) or IQ (Cohen's d = – 0.24, common-language effect size = 0.44; Mann-Whitney test statistic = 225.0, p = 0.4887).

Figure 5 illustrates neuroimaging (FA) differences between the TDC sample and the three subgroups of ASD. The regions with significant differences (after multiple comparison correction) are listed in Additional file 5: Table S3. With the Balanced group, no regional difference survived the multiple comparison correction. The sign of effect size (whether ASD is higher or lower in FA) in Fig. 5 agrees with the sign of DDI values of the subgroups (Advanced > Balanced > Delayed) in most regions; that is, the Advanced group had higher FA values compared with the TDC sample, whereas the Delayed group had lower values. The Balanced subgroup had lower effect sizes compared with other two subgroups. Please note that these results can be partly explained by the fact that the DDI values are indirectly computed from deviation of FA values with respect to the TDC sample; thus, higher FA values are expected for a subgroup with positive DDI values.

Fig. 2 Regional patterns of brain maturation for diffusion (FA, ADC) and anatomical (surface area, volume, thickness) metrics, within **a** TDC and **b** ASD samples. Colors correspond to Pearson correlation (*r*) between age and anatomical/diffusion metrics. All regions are color-coded regardless of their *p* values to better visualize the overall age effects. Note that the brain parcellation used for anatomical metrics included only cortical GM

Beyond the categorical group differences, a dimensional relationship between brain maturation and behavior was also observed within the whole ASD sample. The DDI was significantly correlated with the disorder symptom severity (Spearman $r = -0.20$, CI = [-0.34 to -0.05], $p = 0.0076$). In order to test the robustness of correlation between the DDI and symptom severity to motion during MRI acquisition and IQ, we fit an ordinal regression model to predict ADOS severity scores using the DDI, motion, and total IQ. The DDI had the most dominant contribution in the model (coefficient = -0.32, $p = 0.0166$) followed by IQ (coefficient = -0.01, $p = 0.0264$), and motion was not a significant predictor of severity (coefficient = 0.13, $p = 0.6253$). In other words,
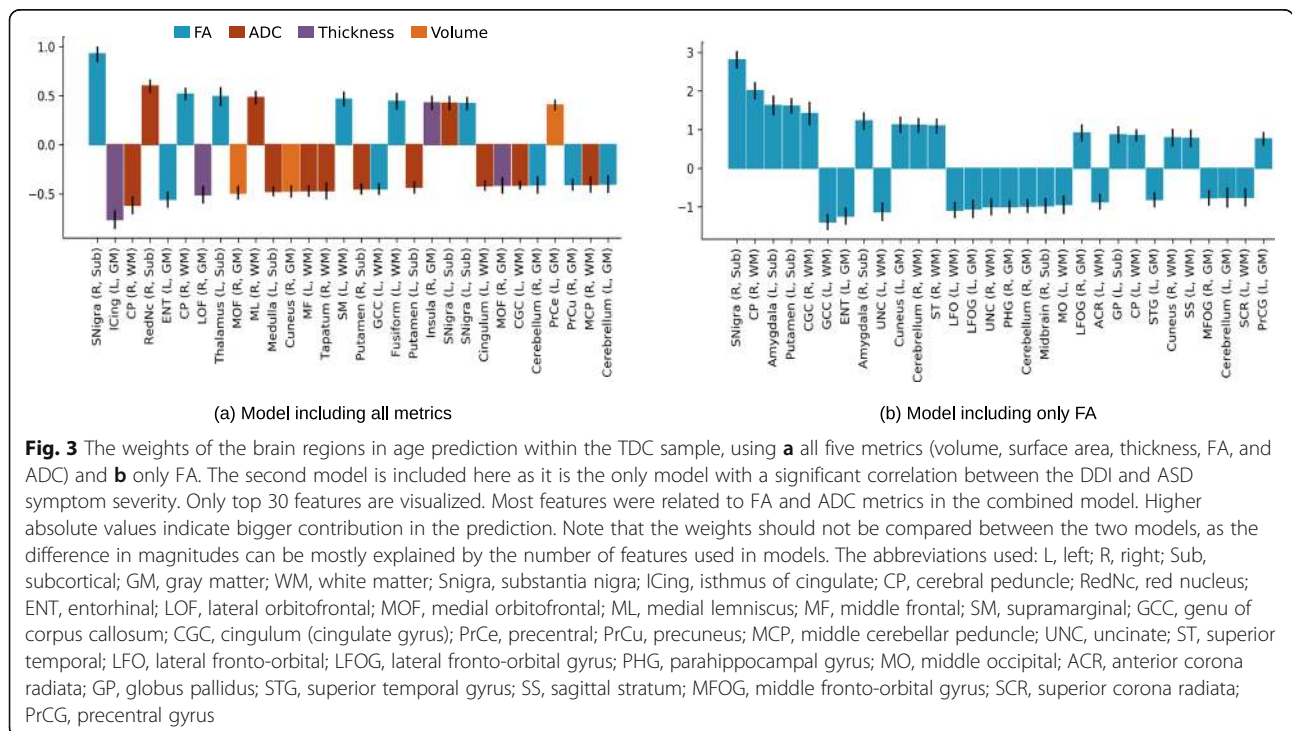

Fig. 3 The weights of the brain regions in age prediction within the TDC sample, using **a** all five metrics (volume, surface area, thickness, FA, and ADC) and **b** only FA. The second model is included here as it is the only model with a significant correlation between the DDI and ASD symptom severity. Only top 30 features are visualized. Most features were related to FA and ADC metrics in the combined model. Higher absolute values indicate bigger contribution in the prediction. Note that the weights should not be compared between the two models, as the difference in magnitudes can be mostly explained by the number of features used in models. The abbreviations used: L, left; R, right; Sub, subcortical; GM, gray matter; WM, white matter; Snigra, substantia nigra; ICing, isthmus of cingulate; CP, cerebral peduncle; RedNc, red nucleus; ENT, entorhinal; LOF, lateral orbitofrontal; MOF, medial orbitofrontal; ML, medial lemniscus; MF, middle frontal; SM, supramarginal; GCC, genu of corpus callosum; CGC, cingulum (cingulate gyrus); PrCe, precentral; PrCu, precuneus; MCP, middle cerebellar peduncle; UNC, uncinate; ST, superior temporal; LFO, lateral fronto-orbital; LFOG, lateral fronto-orbital gyrus; PHG, parahippocampal gyrus; MO, middle occipital; ACR, anterior corona radiata; GP, globus pallidus; STG, superior temporal gyrus; SS, sagittal stratum; MFOG, middle fronto-orbital gyrus; SCR, superior corona radiata; PrCG, precentral gyrus

Table 2 Characteristics of ASD subgroups defined by DDI values

ASD subgroups	Age Mean (Std)	Total IQ Mean (Std)	ADOS CSS Mean (Std)
Delayed	11.53 (3.38)	95.52 (16.41)	8.00 (1.19)
Balanced	12.97 (2.68)	91.27 (24.62)	7.04 (2.08)
Advanced	11.80 (2.13)	99.32 (14.32)	6.47 (1.87)

the correlation between the DDI and symptom severity remained significant when we consider MRI motion and IQ of participants.

Sex differences

In our dataset, the TDC and ASD samples were not matched in sex ratio (see Table 1; χ^2 = 5.49, dof = 1, p = 0.0191). Thus, in order to examine possible contribution of sex differences to the reported results, we compared the DDI values between males and females with ASD. This yielded no notable difference between sexes (Cohen's d = 0.04, common-language effect size = 0.49; Mann-Whitney test statistic = 2322.0, p = 0.8619). We also reran all analyses including only males in both the TDC and ASD samples. The correlation between the DDI and symptom severity was almost identical to the original result above (Spearman r = − 0.20, CI = [− 0.35 to − 0.04], p = 0.0125).

Discussion

In this work, we systematically studied developmental changes on anatomical (surface area, thickness, and volume) and diffusion (FA, ADC) metrics of the brain in normative development and in ASD. We demonstrated diverse age effects in different brain tissue types and regions, depicting a heterogeneous maturation pattern across the whole brain. By fusing these diverse age effects within a multivariate and multimodal machine learning model, we showed that anatomical and diffusion metrics were able to capture brain development with high accuracy. On average, brain maturation patterns, as captured by imaging metrics, were similar between TDC and ASD samples, suggesting preserved core developmental patterns in ASD. On the other hand, at the individual level, deviation from normative development, as computed by the DDI, was significantly correlated with the symptom severity in ASD, highlighting importance of individual-level analysis in disorder samples with heterogeneous presentations.

Regional brain maturation

We reported regional patterns of brain maturation as quantified by correlations between age and several anatomical and diffusion metrics. Our results, showing increased FA and decreased ADC in WM and subcortical regions, agree with previous reports in normative samples [65, 66]. While it is difficult to pinpoint exact mechanisms (e.g., increasing myelination, increasing axonal density, or axonal pruning) yielding these results without detailed microstructural analyses [67], results are
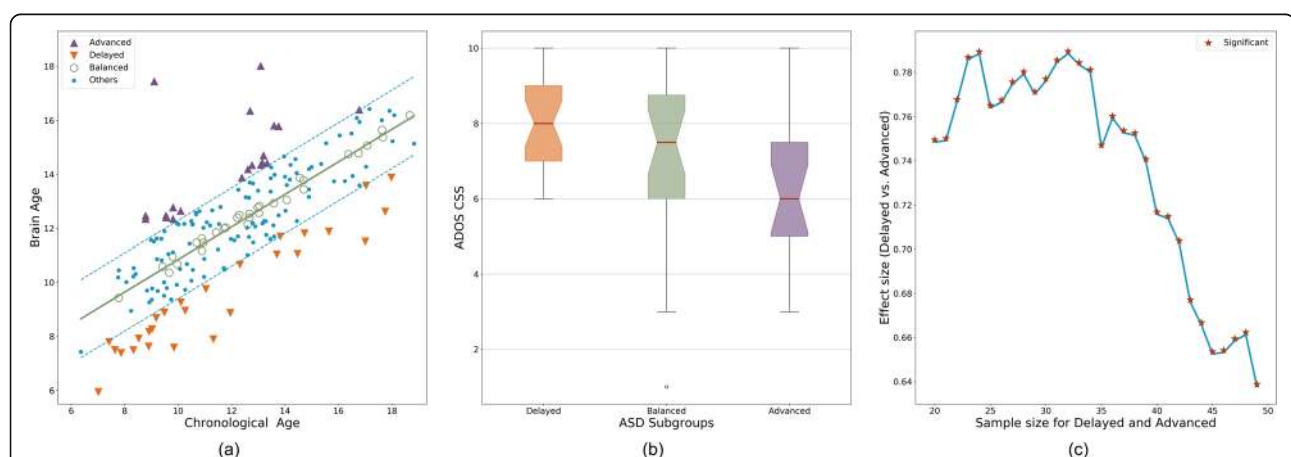

Fig. 4 a Individuals with ASD were grouped into three subgroups based on the DDI values. Advanced group had higher brain age compared with chronological age (DDI > = 1). Delayed group had lower brain age compared with chronological age (DDI < = − 1). Balanced group had similar brain age and chronological age (− 0.2 < DDI < 0.2). **b** ASD severity values for the three subgroups. **c** The effect size of group difference between Advanced and Delayed groups. The effect size is reported as common-language effect size (i.e., probability of having higher severity in the Delayed group), which is an appropriate choice for ordinal severity values. The effect size was calculated for varying number of people in each group (adjusting DDI threshold accordingly) to demonstrate the robustness of group difference to the DDI threshold. Regardless of the sample sizes, the inter-group difference was always significant (p < 0.05)
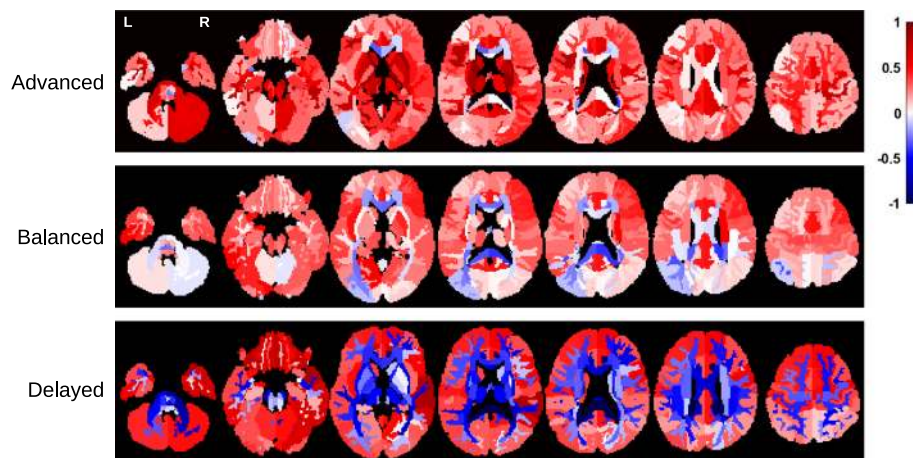
Fig. 5 Neuroimaging (FA) differences between the TDC sample and the three subgroups of ASD, namely Advanced, Balanced, and Delayed. Colors correspond to effect size of group comparison (Cohen's *d*), with positive values indicate higher FA values in ASD. All regions, regardless of *p* values, are visualized. The Advanced group, in average, had higher FA values compared with the TDC sample. The effect sizes become smaller across regions in the Balanced group. In the Delayed group, we see dominantly negative effect sizes. The hierarchy between the subgroups in terms of symptom severity (Delayed > Balanced > Advanced) is preserved (in the reversed direction) with FA values as well

consistent with the expected brain connectivity maturation within the age range of our sample [68, 69]. Notably, both cortical volume and thickness decreased with age. In contrast, cortical surface area did not show a notable change with age; however, this may be due to our use of a linear correlation coefficient, since a few previous studies demonstrated that maturation in anatomical measures follow a cubic or quadratic trend in some areas across this age range [70–72].

We observed age-related differences between the TDC and ASD samples in FA, ADC, and cortical thickness, with small to moderate effect sizes (difference in *r* in the range of 0.13–0.39), although results did not survive multiple comparison correction in our sample, except for ADC in a few regions. Our results, in average, agree with previously reported age-related differences in diffusion [73–77] and anatomical [78–80] metrics in ASD. In our sample, the absolute values of correlation coefficients were decreased in ASD, supporting previous findings of flattened curves of maturation in ASD [73, 76, 79]. The lack of substantial (i.e., not significant after multiple comparison correction) group differences may suggest preserved developmental mechanisms in ASD at the group level; however, this needs further investigations, possibly including nonlinear metrics of correlation. Similar findings, with ASD-related alterations being obscured at the group level while present at the individual level, were reported previously, using a normative modeling approach [81].

Multivariate brain maturation

We observed a diverse effect of maturation in the brain, with effect of age varying across brain tissues and

regions, highlighting the need for using advanced multivariate techniques to better capture inter-regional interactions. Our results with multivariate prediction models (SVR and two other regression models) clearly demonstrated that imaging-based anatomical and diffusion metrics of the brain can effectively capture developmental changes, as suggested by high age prediction accuracy. The tissue microstructure and possibly connectivity-related diffusion measures (ADC and FA) had the highest prediction accuracy, followed by cortical thickness, volume, and surface area. Higher predictive power of diffusion metrics may be due to the age range of our sample, reflecting a specific phase of development when WM matures most. A multimodal prediction model, combining all modalities had the highest prediction accuracy. This was despite the substantial decrease in the number of participants having all metrics and increase in dimensionality, which is known to hurt the prediction performance [82]. These results highlight the complementary nature of anatomical and diffusion metrics, with a relatively higher contribution of diffusion metrics.

In the present study, among the six multivariate models, only one model trained with a single diffusion metric (FA) had a notable correlation between the DDI and symptom severity. On the contrary, the normative model combining all modalities and metrics performed best in age prediction. These two findings, taken together, may suggest that the neuroimaging metrics capture complementary aspects of brain maturation, and ASD-related alterations are mostly linked to a specific aspect that is captured by the FA metric, possibly associated with tissue microstructure and brain connectivity.

Such a hypothesis requires further evaluations with replication studies; nevertheless, it supports the previous reports suggesting links between behavioral profiles in ASD and altered brain diffusion characteristics and connectivity [28, 83, 84]. Indeed, many studies have reported connectivity-related alterations in ASD, suggesting that ASD is a disorder of brain connectivity [85, 86]. Our results expand this conceptualization by suggesting that ASD severity might be related to atypical development in white matter tissue characteristics.

The lack of correlation between symptom severity and the DDI defined by anatomical metrics in our sample should not be taken as a disagreement with previous studies suggesting links between anatomical metrics and behavior [13, 87–89]. It is essential to note that we did not test whether symptom severity correlated with the diffusion and anatomical metrics themselves, or whether the brain measures accurately classified diagnosis. Rather, we tested whether their deviation from the typical development correlated with symptom severity. Given the smaller relationship between age and anatomical measures, particularly surface area, compared with diffusion metrics, it is perhaps unsurprising that the deviation from normative development in these measures does not contain sufficient variation to predict severity. A significant correlation between severity of repetitive behaviors and deviation from normative brain anatomy was reported recently, using another normative modeling approach [81], where each voxel of the brain was analyzed independently. It is possible that aggregating deviations from all voxels and regions into a single score, as done in our approach, may have caused a loss of variation necessary to detect anatomy-behavior relationship. This hypothesis can be tested in future studies by directly comparing different normative modeling approaches within the same sample.

Developmental heterogeneity in ASD
Although regional and global developmental patterns of anatomical and diffusion metrics, on average, were similar between the TDC and ASD samples, our individual-level analysis within the ASD sample revealed significant links between deviation from normative development and disorder symptom severity. We investigated developmental heterogeneity in ASD, by using the DDI to stratify the ASD sample into three developmental subgroups, namely Advanced, Balanced, and Delayed subgroups. We demonstrated a significant hierarchy among the subgroups in terms of mean symptom severity (Advanced < Balanced < Delayed). Going beyond these categorical differences, we also observed a significant correlation between symptom severity and the DDI in the whole ASD sample as well. Our methods and similar stratification techniques can be easily extended to other psychiatric conditions [90] and to other data modalities.

Our results portray a heterogonous picture of ASD, as also suggested by previous studies [91, 92]. Two subgroups of ASD, the Advanced and Delayed subgroups, had neuroimaging differences from the TDC sample in the reversed directions. Within the Advanced group, ASD was associated with higher regional FA values compared with typically development, whereas, lower FA values were present in the Delayed group. Both groups had FA differences in the brain regions previously reported in ASD, such as internal capsule [93–96], external capsule [97, 98], and inferior temporal gyrus [99] in the Advanced group, corpus callosum [95, 97, 100–103], cerebellar peduncle [95, 97, 104], and inferior fronto-occipital fasciculus [98, 100] in the Delayed group, and cingulum [100, 105–107] in both groups. Notably, the regions that showed significant differences were not same for the subgroups. Such a picture supports the idea of *equifinality* in psychiatric disorders [41] that suggests a single behavioral outcome may be linked to distinct underlying mechanisms in different subgroups or even in each individual.

The Advanced group, in average, had less symptom severity not only compared with the Delayed group, but also compared with the Balanced group, which had typical brain age (i.e., close to chronological age). In other words, having advanced brain maturation, which may be considered to be a type of "deviation," is associated with positive outcomes. Previous studies have reported increased cognitive performance for individuals with high brain age, in normative samples [39, 108]. Here we found higher brain age is related to reduced ASD severity. It seems that advanced brain maturation begets positive attributes both in normative and disorder samples. Notably, the Advanced and Delayed subgroups did not differ significantly in terms of IQ scores, and the negative correlation between symptom severity and the DDI remained significant after correcting for IQ differences. Thus, if we wish to speculate a parallel between reduced symptom severity and increased cognitive performance, we should consider cognitive domains that are associated with ASD symptomatology, such as social cognition, executive functioning, and theory of mind [109–114], rather than cognitive domains assessed by standardized IQ measures (i.e., verbal and nonverbal reasoning).

Limitations
Interpretation of the reported results should be made in the light of several limitations of the work. First of all, brain maturation is a dynamic process with different trajectories in different age ranges [20]. Our results only reflect the links between age and certain anatomical and diffusion metrics as observed within the age range of the study sample (6–25 years, mean = 13.0, Std = 3.8). A

comprehensive portrait of the brain development in ASD requires datasets that include a wide range of ages, from infancy to late adulthood. Moreover, our work characterizes brain development only through MRI-based metrics, and their overlap with the underlying biological processes is not well described [115].

We used linear models in order to facilitate better interpretations. More sophisticated yet complicated models could also have been used to possibly have better predictive power, for example, to have higher prediction accuracy in age prediction [116]. Nevertheless, using a simple linear predictor, we were able to achieve a substantial cross-validated accuracy, which effectively demonstrates the capability of our model in capturing the brain maturation patterns.

We performed a cross-sectional analysis to study developmental effects in ASD. More reliable inferences about brain development require longitudinal studies [117] that have the statistical capabilities to better characterize developmental trajectories and to better capture within- and between-person variations [118].

The brain age approach used in this study defines a normative model to predict age from neuroimaging metrics, which is the opposite of other normative modeling approaches that predict neuroimaging metrics from age [38]. The direction of prediction used in brain age approach explicitly defines a normative age model but not a normative model of neuroimaging metrics, which is available only implicitly (e.g., weights of SVR). Although it is always possible to invert the linear mapping between variables to facilitate interpretations on regional neuroimaging metrics, one may also use other normative modeling approaches to achieve this directly [37, 38].

Our results suggested that the DDI derived from only one neuroimaging metric (FA) showed a correlation with symptom severity. Such specific findings necessitate replication studies using other large datasets to demonstrate how these results generalize. Without such replication studies, it is not possible to exclusively attribute ASD-related neuroanatomical alterations to variations in a single diffusion metric.

Based on the reported moderate effect sizes, replication studies using possibly bigger samples are needed for this work to be reliably translated into any clinical decision making or treatment strategies.

Future directions
ASD is a complex psychiatric condition characterized by diverse impairments in multiple domains of functioning [1] and presence of numerous comorbidities including deficits in cognitive function and language ability [119, 120], as well as co-occurring psychiatric and neurological conditions [121]. This complex clinical presentation of the disorder makes it a challenge to quantify the symptom severity using a single measure. Although we used one of the gold-standard measures of symptom severity (ADOS calibrated severity score), a detailed characterization of developmental heterogeneity necessitates studying links between brain development and symptom severity along multiple dimensions. In future work, we will study these multiple dimensions of developmental heterogeneity using our probabilistic data fusion techniques [122].

Our results indicated a notable contribution of diffusion metrics in explaining observed behavioral heterogeneity across development. It seems intuitive to conclude from these results that brain connectivity is a key factor in understanding neurobiological substrates of ASD, which is also supported by previous studies [85, 86]. Nevertheless, diffusion metrics used in this study only characterize the tissue microstructure, but not directly the connectivity between regions. Thus, future studies using direct measures of brain connectivity derived from connectomes [123] (e.g., connectivity strength between regions) are necessary to better understand neurobiological underpinnings of the disorder. Our methods introduced in this study can be easily used in such future studies of brain connectivity.

In future studies, our findings can be extended through use of longitudinal datasets in order to identify diverse trajectories of the DDI across ages. Maturation is a dynamic process; it is expected that an individual with ASD would have differential deviation from the normative brain maturation at different stages of development [20]. Investigations on the DDI dynamics across ages may provide further insights into to our understanding of the individualized pathways of the disorder, especially in relation to different treatment and intervention strategies.

Supplementary information

Additional file 1. Supplementary notes

Additional file 2: Figure S1. Global patterns of brain maturation for diffusion (FA, ADC) and anatomical (surface area, volume, thickness) metrics in ASD. **Figure S2.** Results using Lasso regression. **Figure S3.** Results using Bayesian regression. **Figure S4.** Results using Bayesian regression, with uncertainty is explicitly modeled

Additional file 3: Table S1. Regional brain maturation differences between TDC and ASD samples.

Additional file 4: Table S2. Relationship between DDI and ASD Severity.

Additional file 5: Table S3. Neuroimaging (FA) differences between the TDC sample and the two subgroups of ASD.

Abbreviations
ADC: Apparent diffusion coefficient; ADOS: Autism diagnostic observation schedule; ASD: Autism spectrum disorder; CAR: Center for autism research; CHOP: Children's hospital of Philadelphia; CI: Confidence intervals; CSS: Calibrated severity score; DDI: Developmental deviation index; dMRI: Diffusion magnetic resonance imaging; FA: Fractional anisotropy; FDR: False discovery rate; IRB: Institutional review board; MRI: Magnetic

resonance imaging; RRB: Restricted and repetitive behaviors; SA: Social affect; SVR: Support vector regression; TDC: Typically developing children

Availability of data and materials
All data generated and/or analyzed, and the source code of all computer programs used during this study are available from the corresponding author on reasonable request.

Ethics approval and consent to participate
Data collection and use was approved by the institutional review board (IRB) at Children's Hospital of Philadelphia and the University of Pennsylvania. All participants or their legal guardians gave their consent for research and publication purposes.

Consent for publication
Not applicable.

Competing interests
The authors declare that they have no competing interests.

Author details
[1]Center for Autism Research, The Children's Hospital of Philadelphia, Philadelphia, PA 19104, USA. [2]Department of Biomedical and Health Informatics, The Children's Hospital of Philadelphia, Philadelphia, PA 19104, USA. [3]Department of Psychiatry, University of Pennsylvania, Philadelphia, PA 19104, USA. [4]Center for Biomedical Image Computing and Analytics, University of Pennsylvania, Philadelphia, PA 19104, USA. [5]Department of Psychology, University of Pennsylvania, Philadelphia, PA 19104, USA. [6]DiCIPHR (Diffusion and Connectomics in Precision Healthcare Research) Lab, Department of Radiology, University of Pennsylvania, Philadelphia, PA 19104, USA. [7]Department of Pediatrics, University of Pennsylvania, Philadelphia, PA 19104, USA.

References
1. Levy SE, Mandell DS, Schultz RT. Autism. Lancet. 2009;374(9701):1627–38.
2. Courchesne E. Abnormal early brain development in autism. Mol Psychiatry. 2002;7(S2):S21–3.
3. Piven J, Berthier ML, Starkstein SE, Nehme E, Pearlson G, Folstein S. Magnetic resonance imaging evidence for a defect of cerebral cortical development in autism. Am J Psychiatry. 1990;147(6):734–9.
4. Khundrakpam BS, Lewis JD, Kostopoulos P, Carbonell F, Evans AC. Cortical thickness abnormalities in autism spectrum disorders through late childhood, adolescence, and adulthood: a large-scale MRI study. Cereb Cortex. Mar. 2017;27(3):1721–31.
5. Dichter GS. Functional magnetic resonance imaging of autism spectrum disorders. Dialogues Clin Neurosci. 2012;14(3):319–51.
6. Wolff JJ, et al. Differences in white matter fiber tract development present from 6 to 24 months in infants with autism. Am J Psychiatry. 2012;169(6):589–600.
7. Han J, et al. Development of brain network in children with autism from early childhood to late childhood. Neuroscience. Dec. 2017;367:134–46.
8. Courchesne E, et al. Mapping early brain development in autism. Neuron. 2007;56(2):399–413.
9. Ecker C, Bookheimer SY, Murphy DGM. Neuroimaging in autism spectrum disorder: brain structure and function across the lifespan. Lancet Neurol. 2015;14(11):1121–34.
10. Zielinski BA, et al. Longitudinal changes in cortical thickness in autism and typical development. Brain. 2014;137(6):1799–812.
11. Courchesne E, Carper R, Akshoomoff N. Evidence of brain overgrowth in the first year of life in autism. JAMA. 2003;290(3):337–44.
12. Hazlett HC, et al. Brain volume findings in 6-month-old infants at high familial risk for autism. Am J Psychiatry. 2012;169(6):601–8.
13. Hazlett HC, et al. Early brain development in infants at high risk for autism spectrum disorder. Nature. Feb. 2017;542(7641):348–51.
14. Courchesne E, et al. Unusual brain growth patterns in early life in patients with autistic disorder: an MRI study. Neurology. Jul. 2001;57(2):245–54.
15. Courchesne E. Brain development in autism: early overgrowth followed by premature arrest of growth. Ment Retard Dev Disabil Res Rev. 2004;10(2):106–11.
16. Sacco R, Gabriele S, Persico AM. Head circumference and brain size in autism spectrum disorder: a systematic review and meta-analysis. Psychiatry Res. 2015;234(2):239–51.
17. Stanfield AC, McIntosh AM, Spencer MD, Philip R, Gaur S, Lawrie SM. Towards a neuroanatomy of autism: a systematic review and meta-analysis of structural magnetic resonance imaging studies. Eur Psychiatry. 2008;23(4):289–99.
18. Gotham K, Pickles A, Lord C. Trajectories of autism severity in children using standardized ADOS scores. Pediatrics. 2012;130(5):e1278–84.
19. P. Szatmari, et al., Developmental trajectories of symptom severity and adaptive functioning in an inception cohort of preschool children with autism spectrum disorder, JAMA Psychiatry, vol. 72, no. 3, p. 276, Mar. 2015.
20. Georgiades S, Bishop SL, Frazier T. Editorial perspective: longitudinal research in autism - introducing the concept of 'chronogeneity'. J Child Psychol Psychiatry. 2017;58(5):634–6.
21. Aylward EH, Minshew NJ, Field K, Sparks BF, Singh N. Effects of age on brain volume and head circumference in autism. Neurology. Jul. 2002;59(2):175–83.
22. B. F. Sparks et al., Brain structural abnormalities in young children with autism spectrum disorder, Neurology, vol. 59, no. 2, pp. 184–192, Jul. 2002.
23. C. M. Schumann et al., Longitudinal magnetic resonance imaging study of cortical development through early childhood in autism., J Neurosci, vol. 30, no. 12, pp. 4419–4427, Mar. 2010.
24. Piven J, Arndt S, Bailey J, Havercamp S, Andreasen NC, Palmer P. An MRI study of brain size in autism. Am J Psychiatry. 1995;152(8):1145–9.
25. Courchesne E, Campbell K, Solso S. Brain growth across the life span in autism: age-specific changes in anatomical pathology. Brain Res. 2011;1380:138–45.
26. Barnea-Goraly N, Lotspeich LJ, Reiss AL. Similar white matter aberrations in children with autism and their unaffected siblings. Arch. Gen. Psychiatry. 2010;67(10):1052.
27. Elison JT, et al. White matter microstructure and atypical visual orienting in 7-month-olds at risk for autism. Am J Psychiatry. 2013;170(8):899–908.
28. Ameis SH, et al. A diffusion tensor imaging study in children with ADHD, autism spectrum disorder, OCD, and matched controls: distinct and non-distinct white matter disruption and dimensional brain-behavior relationships. Am J Psychiatry. 2016;173(12):1213–22.
29. Koolschijn PCMP, Caan MWA, Teeuw J, Olabarriaga SD, Geurts HM. Age-related differences in autism: the case of white matter microstructure. Hum Brain Mapp. 2017;38(1):82–96.
30. Zhang F, et al. Whole brain white matter connectivity analysis using machine learning: an application to autism: Neuroimage; 2017.
31. Supekar K, et al. Deficits in mesolimbic reward pathway underlie social interaction impairments in children with autism. Brain. 2018;141(9):2795–805.
32. d'Albis M-A, et al. Local structural connectivity is associated with social cognition in autism spectrum disorder. Brain. 2018;141(12):3472–81.
33. Mengotti P, et al. Altered white matter integrity and development in children with autism: a combined voxel-based morphometry and diffusion imaging study. Brain Res Bull. 2011;84(2):189–95.
34. Jou RJ, Reed HE, Kaiser MD, Voos AC, Volkmar FR, Pelphrey KA. White matter abnormalities in autism and unaffected siblings. J Neuropsychiatry Clin Neurosci. 2016;28(1):49–55.

35. Basser PJ, Jones DK. Diffusion-tensor MRI: theory, experimental design and data analysis - a technical review. NMR Biomed. 2002;15(7–8):456–67.
36. Assemlal H-E, Tschumperlé D, Brun L, Siddiqi K. Recent advances in diffusion MRI modeling: angular and radial reconstruction. Med Image Anal. Aug. 2011;15(4):369–96.
37. Marquand AF, Kia SM, Zabihi M, Wolfers T, Buitelaar JK, Beckmann CF. Conceptualizing mental disorders as deviations from normative functioning. Mol Psychiatry. 2019;24(10):1415–24.
38. Marquand AF, Rezek I, Buitelaar J, Beckmann CF. Understanding heterogeneity in clinical cohorts using normative models: beyond case-control studies. Biol Psychiatry. 2016;80(7):552–61.
39. Erus G, et al. Imaging patterns of brain development and their relationship to cognition. Cereb Cortex. 2015;25(6):1676–84.
40. Wolfers T, et al. Mapping the heterogeneous phenotype of schizophrenia and bipolar disorder using normative models. JAMA Psychiatry. 2018;75(11):1146.
41. Cicchetti D, Rogosch FA. Equifinality and multifinality in developmental psychopathology. Dev Psychopathol. 1996;8(4):597–600.
42. Franke K, Ziegler G, Klöppel S, Gaser C, Initiative A's DN. Estimating the age of healthy subjects from T1-weighted MRI scans using kernel methods: exploring the influence of various parameters. Neuroimage. 2010;50(3):883–92.
43. Cole JH, et al. Predicting brain age with deep learning from raw imaging data results in a reliable and heritable biomarker. Neuroimage. 2017;163:115–24.
44. American Psychiatric Association, Diagnostic and Statistical Manual of Mental Disorders, 4th Edition, Text Revision (DSM-IV-TR). Washington, D.C: American Psychiatric Publishing, 2000.
45. Lord C, et al. The autism diagnostic observation schedule-generic: a standard measure of social and communication deficits associated with the spectrum of autism. J Autism Dev Disord. 2000;30(3):205–23.
46. Rutter M, Le Couteur A, Lord C. Autism diagnostic interview-revised (ADI-R). Los Angeles, CA: Western Psychological Services; 2003.
47. Gotham K, Pickles A, Lord C. Standardizing ADOS scores for a measure of severity in autism spectrum disorders. J Autism Dev Disord. 2009; 39(5):693–705.
48. C. Elliot, The differential abilities scale, Second Edition. Harcourt Assessments, Inc., 2007.
49. Tustison NJ, et al. N4ITK: improved N3 Bias correction. IEEE Trans Med Imaging. 2010;29(6):1310–20.
50. Shi F, Wang L, Dai Y, Gilmore JH, Lin W, Shen D. LABEL: pediatric brain extraction using learning-based meta-algorithm. Neuroimage. 2012;62(3): 1975–86.
51. "FreeSurfer." [Online]. Available: https://surfer.nmr.mgh.harvard.edu/fswiki/DownloadAndInstall5.3. [Accessed: 08-Dec-2019].
52. Desikan RS, et al. An automated labeling system for subdividing the human cerebral cortex on MRI scans into gyral based regions of interest. Neuroimage. 2006;31(2):968-80.
53. Power JD, Barnes KA, Snyder AZ, Schlaggar BL, Petersen SE. Spurious but systematic correlations in functional connectivity MRI networks arise from subject motion. Neuroimage. 2012;59(3):2142–54.
54. Smola AJ, Schölkopf B. A tutorial on support vector regression. Stat Comput. 2004;14(3):199–222.
55. Koutsouleris N, et al. Use of neuroanatomical pattern regression to predict the structural brain dynamics of vulnerability and transition to psychosis. Schizophr Res. 2010;123(2–3):175–87.
56. Pedregosa F, et al. Scikit-learn: machine learning in Python. J Mach Learn Res. 2011;12:2825–30.
57. G. Rossum, Python reference manual, CWI (Centre for Mathematics and Computer Science), Amsterdam, 1995.
58. Galton F. Regression towards mediocrity in hereditary stature. J Anthropol Inst Gt Britain Irel. 1886;15:246–63.
59. Smith SM, Vidaurre D, Alfaro-Almagro F, Nichols TE, Miller KL. Estimation of brain age delta from brain imaging. Neuroimage. 2019;200:528–39.
60. McGraw KO, Wong SP. A common language effect size statistic. Psychol Bull. 1992;111(2):361–5.
61. Brooks ME, Dalal DK, Nolan KP. Are common language effect sizes easier to understand than traditional effect sizes? J Appl Psychol. 2014;99(2):332–40.
62. Benjamini Y, Hochberg Y. Controlling the false discovery rate: a practical and powerful approach to multiple testing. J R Stat Soc Ser B. 1995;57(1): 289–300.
63. R. H. B. Christensen, ordinal---regression models for ordinal data, 2018.
64. R Core Team, R: a language and environment for statistical computing. Vienna, Austria, 2017.
65. Qiu D, Tan L-H, Zhou K, Khong P-L. Diffusion tensor imaging of normal white matter maturation from late childhood to young adulthood: voxel-wise evaluation of mean diffusivity, fractional anisotropy, radial and axial diffusivities, and correlation with reading development. Neuroimage. 2008; 41(2):223–32.
66. Simmonds DJ, Hallquist MN, Asato M, Luna B. Developmental stages and sex differences of white matter and behavioral development through adolescence: a longitudinal diffusion tensor imaging (DTI) study. Neuroimage. 2014;92:356–68.
67. Raffelt DA, et al. Investigating white matter fibre density and morphology using fixel-based analysis. Neuroimage. 2017;144(Pt A):58–73.
68. Lebel C, Beaulieu C. Longitudinal development of human brain wiring continues from childhood into adulthood. J Neurosci. 2011;31(30): 10937–47.
69. Blakemore S-J. Imaging brain development: the adolescent brain. Neuroimage. 2012;61(2):397–406.
70. Giedd JN, et al. Brain development during childhood and adolescence: a longitudinal MRI study. Nat Neurosci. 1999;2(10):861–3.
71. Ducharme S, et al. Trajectories of cortical surface area and cortical volume maturation in normal brain development. Data Br. 2015;5:929–38.
72. Tamnes CK, et al. Development of the cerebral cortex across adolescence: a multisample study of inter-related longitudinal changes in cortical volume, surface area, and thickness. J Neurosci. 2017;37(12): 3402–12.
73. Cheng Y, Chou K-H, Chen I-Y, Fan Y-T, Decety J, Lin C-P. Atypical development of white matter microstructure in adolescents with autism spectrum disorders. Neuroimage. 2010;50(3):873–82.
74. Bakhtiari R, et al. Differences in white matter reflect atypical developmental trajectory in autism: a tract-based spatial statistics study. NeuroImage Clin. 2012;1(1):48–56.
75. Mak-Fan KM, Morris D, Vidal J, Anagnostou E, Roberts W, Taylor MJ. White matter and development in children with an autism spectrum disorder. Autism. 2013;17(5):541–57.
76. Ouyang M, et al. Atypical age-dependent effects of autism on white matter microstructure in children of 2-7 years. Hum Brain Mapp. 2016;37(2):819–32.
77. Kleinhans NM, et al. Age-related abnormalities in white matter microstructure in autism spectrum disorders. Brain Res. 2012;1479:1–16.
78. Libero LE, DeRamus TP, Deshpande HD, Kana RK. Surface-based morphometry of the cortical architecture of autism spectrum disorders: volume, thickness, area, and gyrification. Neuropsychologia. 2014;62:1–10.
79. Raznahan A, et al. Cortical anatomy in autism spectrum disorder: an in vivo MRI study on the effect of age. Cereb Cortex. 2010;20(6):1332–40.
80. van Rooij D, et al. Cortical and subcortical brain morphometry differences between patients with autism Spectrum disorder and healthy individuals across the lifespan: results from the ENIGMA ASD working group. Am J Psychiatry. 2018;175(4):359–69.
81. Zabihi M, et al. Dissecting the heterogeneous cortical anatomy of autism spectrum disorder using normative models. Biol Psychiatry Cogn Neurosci Neuroimaging. 2019;4(6):567–78.
82. Trunk GV. A problem of dimensionality: a simple example. IEEE Trans Pattern Anal Mach Intell. 1979;PAMI-1(3):306–7.
83. Noriuchi M, et al. Altered white matter fractional anisotropy and social impairment in children with autism spectrum disorder. Brain Res. 2010;1362:141–9.
84. Lin H-Y, et al. Development of frontoparietal connectivity predicts longitudinal symptom changes in young people with autism spectrum disorder. Transl. Psychiatry. 2019;9(1):86.
85. Minshew NJ, Williams DL. The new neurobiology of autism. Arch. Neurol. 2007;64(7):945.
86. Wass S. Distortions and disconnections: disrupted brain connectivity in autism. Brain Cogn. 2011;75(1):18–28.
87. Langen M, Bos D, Noordermeer SDS, Nederveen H, van Engeland H, Durston S. Changes in the development of striatum are involved in repetitive behavior in autism. Biol Psychiatry. 2014;76(5):405–11.
88. Moradi E, Khundrakpam B, Lewis JD, Evans AC, Tohka J. Predicting symptom severity in autism spectrum disorder based on cortical thickness measures in agglomerative data. Neuroimage. 2017;144(Pt A):128–41.
89. Prigge MBD, et al. Social responsiveness scale (SRS) in relation to longitudinal cortical thickness changes in autism Spectrum disorder. J Autism Dev Disord. 2018;48(10):3319–29.

Tunç *et al. Molecular Autism*   (2019) 10:46

Page 14 of 14

90. Koutsouleris N, et al. Accelerated brain aging in schizophrenia and beyond: a neuroanatomical marker of psychiatric disorders. Schizophr Bull. 2014; 40(5):1140–53.
91. Betancur C. Etiological heterogeneity in autism spectrum disorders: more than 100 genetic and genomic disorders and still counting. Brain Res. 2011; 1380:42–77.
92. Jeste SS, Geschwind DH. Disentangling the heterogeneity of autism spectrum disorder through genetic findings. Nat Rev Neurol. 2014;10(2):74–81.
93. McLaughlin K, et al. Longitudinal development of thalamic and internal capsule microstructure in autism spectrum disorder. Autism Res. 2018;11(3):450–62.
94. Mitelman SA, et al. Increased white matter metabolic rates in autism spectrum disorder and schizophrenia. Brain Imaging Behav. 2018;12(5): 1290–305.
95. Shukla DK, Keehn B, Lincoln AJ, Müller R-A. White matter compromise of callosal and subcortical fiber tracts in children with autism spectrum disorder: a diffusion tensor imaging study. J. Am. Acad. Child Adolesc. Psychiatry. 2010;12:1269–78.
96. J. E. Villalón-Reina et al., Altered white matter microstructure in 22q11.2 deletion syndrome: a multisite diffusion tensor imaging study Mol. Psychiatry, 2019.
97. Dougherty CC, Evans DW, Myers SM, Moore GJ, Michael AM. A comparison of structural brain imaging findings in autism spectrum disorder and attention-deficit hyperactivity disorder. Neuropsychol Rev. 2016;26(1):25–43.
98. Saaybi S, et al. Pre- and post-therapy assessment of clinical outcomes and white matter integrity in autism Spectrum disorder: pilot study. Front Neurol. 2019;10:877.
99. Billeci L, et al. Brain network organization correlates with autistic features in preschoolers with autism spectrum disorders and in their fathers: preliminary data from a DWI analysis. J. Clin. Med. 2019;8(4):487.
100. Jou RJ, Jackowski AP, Papademetris X, Rajeevan N, Staib LH, Volkmar FR. Diffusion tensor imaging in autism Spectrum disorders: preliminary evidence of abnormal neural connectivity. Aust New Zeal J Psychiatry. 2011; 45(2):153–62.
101. Sui YV, Donaldson J, Miles L, Babb JS, Castellanos FX, Lazar M. Diffusional kurtosis imaging of the corpus callosum in autism. Mol. Autism. 2018;9(1):62.
102. Fingher N, et al. Toddlers later diagnosed with autism exhibit multiple structural abnormalities in temporal corpus callosum fibers. Cortex. 2017;97: 291–305.
103. Alexander AL, et al. Diffusion tensor imaging of the corpus callosum in autism. Neuroimage. 2007;34(1):61–73.
104. Hanaie R, et al. Altered microstructural connectivity of the superior cerebellar peduncle is related to motor dysfunction in children with autistic spectrum disorders. Cerebellum. 2013;12(5):645–56.
105. Bubb EJ, Metzler-Baddeley C, Aggleton JP. The cingulum bundle: anatomy, function, and dysfunction. Neurosci Biobehav Rev. 2018;92:104–27.
106. Ikuta T, et al. Abnormal cingulum bundle development in autism: a probabilistic tractography study. Psychiatry Res Neuroimaging. 2014;221(1):63–8.
107. Hau J, Aljawad S, Baggett N, Fishman I, Carper RA, Müller R. The cingulum and cingulate U-fibers in children and adolescents with autism spectrum disorders. Hum Brain Mapp. 2019;40(11):3153–64.
108. Ullman H, Klingberg T. Timing of white matter development determines cognitive abilities at school entry but not in late adolescence. Cereb Cortex. 2016;27(9):4516–22.
109. Frith U, Happé F. Autism: beyond theory of mind. Cognition. 1994;50(1–3): 115–32.
110. Boyd BA, McBee M, Holtzclaw T, Baranek GT, Bodfish JW. Relationships among repetitive behaviors, sensory features, and executive functions in high functioning autism. Res Autism Spectr Disord. 2009;3(4):959–66.
111. Gilotty L, Kenworthy L, Sirian L, Black DO, Wagner AE. Adaptive skills and executive function in autism Spectrum disorders. Child Neuropsychol. 2002; 8(4):241–8.
112. Leung RC, Vogan VM, Powell TL, Anagnostou E, Taylor MJ. The role of executive functions in social impairment in autism Spectrum disorder. Child Neuropsychol. 2016;22(3):336–44.
113. Henderson HA, et al. Self-referenced memory, social cognition, and symptom presentation in autism. J Child Psychol Psychiatry. 2009;50(7):853–61.
114. Bishop-Fitzpatrick L, Mazefsky CA, Eack SM, Minshew NJ. Correlates of social functioning in autism Spectrum disorder: the role of social cognition. Res Autism Spectr Disord. 2017;35:25–34.
115. Jones DK, Knösche TR, Turner R. White matter integrity, fiber count, and other fallacies: the do's and don'ts of diffusion MRI. Neuroimage. 2013;73:239–54.
116. Amoroso N, et al. Deep learning and multiplex networks for accurate modeling of brain age. Front Aging Neurosci. 2019;11:115.
117. Lange N, et al. Longitudinal volumetric brain changes in autism spectrum disorder ages 6-35 years. Autism Res. 2015;8(1):82–93.
118. Snedecor GW, Cochran WG. Statistical methods, eight. Ames, Iowa: Iowa state University press; 1989.
119. Christensen DL, et al. Prevalence and characteristics of autism Spectrum disorder among children aged 8 years--autism and developmental disabilities monitoring network, 11 sites, United States, 2012. MMWR Surveill Summ. 2016;65(3):1–23.
120. Kjelgaard MM, Tager-Flusberg H. An investigation of language impairment in autism: implications for genetic subgroups. Lang Cogn Process. 2001; 16(2–3):287–308.
121. Simonoff E, Pickles A, Charman T, Chandler S, Loucas T, Baird G. Psychiatric disorders in children with autism spectrum disorders: prevalence, comorbidity, and associated factors in a population-derived sample. J Am Acad Child Adolesc Psychiatry. 2008;47(8):921–9.
122. Tunc B, et al. PUNCH: population characterization of heterogeneity. Neuroimage. 2014;98:50–60.
123. Ingalhalikar M, et al. Sex differences in the structural connectome of the human brain. Proc Natl Acad Sci U S A. 2014;111(2):823–8.

Publisher's Note